ADVANCED FUNCTIONAL MATERIALS
www.afm-journal.de

Materials Views
www.MaterialsViews.com

Liquid-Phase Exfoliation of Nanotubes and Graphene

By *Jonathan N. Coleman**

Many applications of carbon nanotubes require the exfoliation of the nanotubes to give individual tubes in the liquid phase. This requires the dispersion, exfoliation, and stabilization of nanotubes in a variety of liquids. In this paper recent work in this area is reviewed, focusing on results from the author's group. It begins by reviewing stabilization mechanisms before exploring research into the exfoliation of nanotubes in solvents, by using surfactants or biomolecules and by covalent attachment of molecules. The concentration dependence of the degree of exfoliation in each case will be highlighted. In addition research into the dispersion mechanism for each dispersant type is discussed. Most importantly, dispersion quality metrics for all dispersants are compared. From this analysis, it is concluded that functionalized nanotubes can be exfoliated to the greatest degree. Finally, the extension of this work to the liquid phase exfoliation of graphite to give graphene is reviewed.

1. Introduction

Low-dimensional nanostructured materials such as carbon nanotubes[1] or graphene[2,3] are potentially useful in many areas of nanoscience and nanotechnology. For example, single-walled carbon nanotubes (SWNTs) have mechanical,[4,5]electrical,[6] and thermal[7] properties unheard of in any other material. They are extremely stiff, displaying Young's modulus close to 1 TPa, and are among the world's strongest materials, with strength between 50 and 100 GPa.[4] Nanotubes are predicted to have very large thermal conductivity of up to 6 000 $W\,mK^{-1}$.[8–10] While this has not yet been attained, values around 3000 $W\,mK^{-1}$ have been measured for multiwalled nanotubes.[7] In addition, nanotubes can display semiconducting or metallic properties depending on how they are rolled up. Due to their one dimensionality, they can carry extremely large current densities of up to 100 $MA\,cm^{-2}$,[6] with carrier mobilities as high as $10^5\ cm^2\,V^{-1}\,s^{-1}$ having been observed in semiconducting nanotubes.[11] Such properties make nanotubes ideal for use as transistors or interconnects and in logic circuits.[12,13]

However, while most of these properties are associated with isolated, individual nanotubes, isolated SWNTs are rarely available to experimentalists. They tend to aggregate into large ropes or bundles due to attractive van der Waals interactions. These bundles can be tens of nanometers in diameter and many micrometers long and contain huge numbers of both metallic and semiconducting SWNT tubes. Bundle properties are inferior to those of isolated SWNTs. It is non-trivial to separate SWNTs from bundles, making this issue a serious hurdle to real applications.[5,14,15]

The most common method to separate nanotubes from their bundles is liquid phase exfoliation and stabilization of nanotubes. Such stabilization cannot be successful unless the attractive inter-nanotube potential is balanced by a repulsive potential. Various methods to provide this repulsive potential have been explored. Nanotubes have been dispersed and stabilized with the aid of specific solvents,[16–24] acids,[25,26] macromolecules,[27–30] and surfactants,[31–34] as well as through covalent functionalization strategies.[35,36] Such systems have been characterized by a range of techniques such as atomic force microscopy,[37] infra-red photoluminescence and absorbance spectroscopy,[34] viscometry,[25] and small angle neutron scattering,[32] to name but a few. These strategies have been extremely successful, resulting in highly exfoliated, well-defined and comprehensively characterized systems of dispersed nanotubes.[38–40]

The discovery of graphene in 2004 gave us a new low-dimensional carbon-based nanomaterial to explore.[2,3] Even more so than with nanotubes, the success of graphene research depends on the exfoliation of graphene from its parent crystal. While this was initially achieved by micromechanical cleavage, it soon became apparent that the sort of strategies used to exfoliate nanotubes in the liquid phase could be successfully applied to graphene.[41–44]

In this paper we review the work carried out in our group on the liquid-phase dispersion of nanotubes and graphene. We first consider the mechanisms for stabilization of nanotubes (which also apply to graphene). Then we will review the work carried out in our group on nanotube stabilization in solvents, using surfactants or biomolecules and by covalent functionalization. Finally, we will discuss recent work on the exfoliation of graphene in the liquid phase. We note that in all cases in this work, the term ''nanotubes'' refers to single-walled nanotubes.

2. Background Theory

Users usually encounter carbon nanotubes as a powder, bought from a commercial supplier. Nanotubes have a tendency to aggregate into bundles, which themselves agglomerate to form larger aggregates to make up this powder. The fundamental reason

[*] Prof. J. N. Coleman
School of Physics and CRANN
Trinity College Dublin
Dublin 2 (Ireland)
E-mail: colemaj@tcd.ie

DOI: 10.1002/adfm.200901640

for the mutual attraction between nanotubes is the presence of van der Waals (dispersive) interactions between carbon atoms in adjacent nanotubes. The potential energy associated with these pairwise interactions is just $V(r) = -C/r^6$, where r is the inter-atomic separation and C is a constant (see below).[45] However, the total interaction between nearby nanotubes is the sum of all pairwise interactions counted over all atoms. The result of this summation depends on the separation and angle between the nanotubes. We present the limiting cases for crossed and aligned nanotubes, calculated for simplicity by modeling the nanotubes as solid cylinders. For nanotubes of length, L, radius, R, and separated by a distance, D, the interaction potentials are:[45]

$$V(D) = -\frac{AL\sqrt{R}}{24D^{3/2}} \quad \text{Aligned} \tag{1a}$$

$$V(D) = -\frac{AR}{6D} \quad \text{Crossed} \tag{1b}$$

Here, A is the Hamaker constant which is given by $A = \pi^2\rho^2C$ in vacuum, where ρ is the number of atoms per unit volume in the cylinders. Note these potentials are of much longer range than the atom–atom pairwise interactions.

These type of attractive potentials are always present, although their strength can be modified in a liquid environment depending on the relative values of the cylinder and liquid dielectric properties (see below).[45] If their effects are not addressed, nearby nanotubes will always tend to aggregate. Thus, dispersion of nanotubes in the liquid phase involves controlling the overall liquid/nanotube system in order to counteract the attractive potentials described above.

2.1. Energetics of Nanotube Dispersion in Solvents

The simplest way to disperse nanotubes is in suitable solvents. However, nanotubes cannot be stably dispersed in any solvent. For the vast majority of solvents, forced dispersion, using ultrasound for example, is rapidly followed by aggregation and sedimentation. Thus, it is important to understand what differentiates a good solvent from a bad solvent. To achieve this we must understand the energetics of the solvent–nanotube interaction.

For simplicity we can apply standard solution theory, considering the nanotubes as large solute molecules.[45–48] We first consider how the attractive inter-nanotube potential is modified by the presence of solvent. In vacuum, the dispersive inter-atomic potential felt by two identical atoms is given by the London equation:[45]

$$V(r) = -\frac{3}{4}\frac{I\alpha_0^2}{(4\pi\varepsilon_0)^2 r^6} \tag{2}$$

where I is the ionization potential of the atoms and α_0 is the atom's polarizability. McLachlan has shown that in the presence of a solvent, this expression is significantly modified:[45,49]

$$V(r) = -\frac{\sqrt{3}I}{4}\frac{a^6}{r^6}\frac{\left(n_A^2 - n_B^2\right)^2}{\left(n_A^2 + 2n_B^2\right)^{3/2}} \tag{3}$$

Jonathan Coleman obtained both his BA and PhD from Trinity College Dublin. Since 2001 he has been a Lecturer and then Associate Professor in the School of Physics in Trinity College Dublin. He is also a Principle Investigator in the CRANN Institute. His research focuses on dispersion and exfoliation of low dimensional nanostructures. This research is then used to develop functional composites and conducting thin films.

Here, the solute molecules are modeled as spheres of radius a while the solute and solvent are described by their refractive indices, n_A and n_B, respectively. Similarly, in the presence of a solvent, the Hamaker constant (dispersion interaction only) is modified to

$$A = \frac{3I}{16\sqrt{2}}\frac{\left(n_A^2 - n_B^2\right)^2}{\left(n_A^2 + n_B^2\right)^{3/2}} \tag{4}$$

For example, in the case of hydrocarbons dispersed in water, A is reduced by more than an order of magnitude compared to those separated by vacuum.[45]

The important thing to note about Equations 3 and 4 is the $(n_A^2 - n_B^2)$ part. Because of this, $V(r)$ and A both approach zero as n_B approaches n_A. This means that perfect matching of n_A and n_B will result in no attractive potential and so no solute aggregation, resulting in excellent dispersion. This is the basis of the "like dissolves like" rule in chemistry. Thus Equations 3 and 4 allow us to think of n_B and n_A as solubility parameters. These are parameters which allow the identification of solvents for a given solute.

This principle is usually expressed slightly differently. Generally, in addition to solute–solvent interactions, one considers solute–solute and solvent–solvent interactions. The key factor is the strength of the solute–solvent interaction relative to the inter-solute and inter-solvent interactions. If the solute–solvent interaction is strong, it will cost energy to bring solute molecules (nanotubes) together in the solvent, as this will displace solvent molecules at the solvent–solute (solvent–nanotube) interface. In this scenario, if solute molecules aggregate, the result is an increase in energy. This is equivalent to the presence of a short range repulsive interaction.[48]

In Flory–Huggins theory, we describe the balance of these interaction energies by the Flory–Huggins parameter, χ.[47,48] For mixtures of small molecules, where solute and solvent molecular volumes are similar, χ is defined as:

$$\chi = -\frac{z}{2}\frac{(2\varepsilon_{AB} - \varepsilon_{AA} - \varepsilon_{BB})}{kT} \tag{5}$$

where z is the coordination number of both solvent and solute and ε represents the strength of the inter-molecule pairwise interaction energy (taken as a positive number). The subscripts A and B represent the solute and solvent respectively. While care

must be taken applying Equation 5 to large structures such as nanotubes, the form of this expression makes clear the meaning of χ. If $\chi < 0$, solute–solvent interactions are dominant, while if $\chi > 0$, the solute molecules (nanotubes) are attracted to each other.

We generally measure the energetic cost of mixing solute and solvent by the enthalpy of mixing, $\Delta\overline{H}_{mix}$:[19,48]

$$\Delta\overline{H}_{mix} = \chi\phi(1-\phi)kT/v_0 \quad (6)$$

Here $\Delta\overline{H}_{mix}$ is the enthalpy of mixing per unit volume of solvent, while ϕ is the solute volume fraction and v_0 is the solvent molecular volume. Clearly, the smaller χ is, the smaller $\Delta\overline{H}_{mix}$ is and so the more favourable mixing is. A closely related expression is the Hildebrand–Scratchard expression, which can be written as:[19,48]

$$\Delta\overline{H}_{mix} \approx (\delta_{T,A} - \delta_{T,B})^2\phi(1-\phi) \quad (7)$$

where $\delta_{T,A}$ and $\delta_{T,B}$ are the Hildebrand solubility parameters of the solute and solvent respectively. It should be noted that Equation 7 is approximate. Use of the geometric mean approximation in the derivation results in the spurious prediction of only positive values of $\Delta\overline{H}_{mix}$.[46,47] The value of this expression is that it clearly shows that dispersion is favored when the solubility parameters of solvent and solute match. The solubility parameter of a material is easily found as it is just the square root of the (total) cohesive energy density ($E_{C,T}/V$) of the material: $\delta_T = \sqrt{E_{C,T}/V}$. Note that it can be shown that Equation 3 can be modified to take a similar form to Equation 7: $V(r) \propto -(\delta_{T,A} - \delta_{T,B})^2 r^6$, showing the link between solubility parameters and interatomic potentials.[45]

We note that Equation 7 only takes into account dispersive contributions to the cohesive energy density. In reality most systems also display polar and hydrogen bonding interactions. This leads to three solubility parameters, each one equal to the square root of the associated cohesive energy density.[19,46] These are the Hansen solubility parameters, and the sum of their squares equals the square of the Hildebrand solubility parameter, δ_T:

$$\delta_T^2 = \delta_D^2 + \delta_P^2 + \delta_H^2 \quad (8)$$

where δ_D, δ_P, and δ_H are the dispersive, polar, and Hydrogen bonding solubility parameters. Within this new scheme we can write the Flory–Huggins parameter as[19,46]

$$\chi \approx \frac{v_0}{kT}\left[(\delta_{D,A} - \delta_{D,B})^2 + (\delta_{P,A} - \delta_{P,B})^2 + (\delta_{H,A} - \delta_{H,B})^2\right] \quad (9)$$

This means that to minimize the energetic cost of dispersion, all three solubility parameters of the solvent must match those of the solute.

We note that in solubility theory, a dispersion can be considered a solution when the free energy of mixing is negative. The free energy of mixing, $\Delta\overline{G}_{mix}$, is given by

$$\Delta\overline{G}_{mix} = \Delta\overline{H}_{mix} - T\Delta\overline{S}_{mix} \quad (10)$$

where $\Delta\overline{S}_{mix}$ is the entropy of mixing per unit volume. For many systems, a large entropy of mixing ensures a negative free energy of mixing. However, nanotubes are big and rigid so the entropy of mixing is generally small.[19] This is critically important because in this case the $\Delta\overline{S}_{mix}$ term in Equation 10 cannot be relied upon to minimize $\Delta\overline{G}_{mix}$. Thus, systems where nanotubes are well dispersed are likely to be those with small $\Delta\overline{H}_{mix}$. Ultimately, this means good solvents for nanotubes should be those with the correct Hansen parameters.

2.2. Surfactant Stabilization: DLVO Theory

Stabilization of colloids often relies on the presence of a surface charge.[45,50] This may be due to deprotonation of surface groups or adsorption of ions from the solvent. This surface charge then attracts a diffuse layer of counter-ions from the liquid to form an electric double layer. Because of the diffuse nature (due to Brownian motion) of the counter-ions, the overall result is an effective surface charge, resulting in Coulomb repulsion between nearby charged colloids.[45,50] We can apply this to carbon nanotubes, introducing a temporary and removable surface charge, by allowing surfactant molecules to adsorb onto nanotubes via their hydrophobic tails. Usually an ion, often Na^+ or Li^+, becomes dissociated from the hydrophilic head groups and acts as the counter-ion. The adsorbed molecular ions then interact with the solvent (water).

The important point here is that the diffuse cloud of counter ions are spatially separated from the tail group molecular ions. This arrangement acts as a multi-pole. Put simply, from afar the surfactant-coated nanotube appears to carry an effective charge. We indicate the magnitude and sign of the effective charge associated with the double layer through the zeta potential, ζ. This is the electrostatic potential at the edge of the layer of bound tail groups.

The presence of the double layer means that the attractive van der Waals potential due to the nanotubes is balanced by the repulsive potential associated with the double layer. The physics of the double layer was first studied by Derjaguin and Landau and independently by Verwey and Overbeek and is known as DLVO theory.[45,50] The repulsive potential depends on the geometric properties of the charged surface but generally takes the form $V(D) = Be^{-\kappa D}$. Here κ^{-1} is called the Debye screening length and is a measure of the thickness of the double layer. In general, B depends on κ, ζ, and the geometric properties of the surface and takes quite a complex form in the case of cylinders.[51]

Thus the total interaction potential experienced by nearby nanotubes has an attractive (van der Waals) term and a repulsive (DLVO) term. For crossed nanotubes, this is:

$$V_T(D) = -\frac{AR}{6D} + Be^{-\kappa D} \quad (11)$$

The form of this potential is shown in Figure 1. The attractive part dominates at low nanotube separation, resulting in a deep potential well at very low D. However at intermediate D, the potential increases, resulting in a potential barrier, before falling again as D becomes large. It is this potential barrier that stabilizes the surfactant-coated nanotubes against aggregation. The higher the barrier, the more stable the system. In general, the height of the

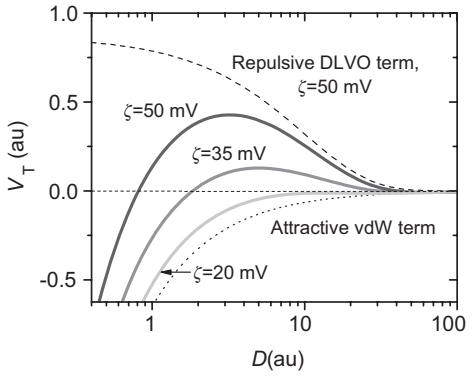

Figure 1. Graph showing repulsive (DLVO) and attractive (van der Waals) components of the potential energy experienced by pairs of surfactant coated nanotubes (dashed lines). The solid lines represent the total potential energy for different values of the zeta potential.

barrier scales monotonically with the zeta potential (we note that κ, which depends on the surfactant concentration, $\kappa \propto \sqrt{C_{surf}}$, also effects the barrier height such that high C_{surf} lowers the barrier height, see Refs. [45,50]).

Thus, when dispersing nanotubes using surfactants, it is critical to chose the surfactant type and concentration such that ζ and κ are optimized to maximize the potential barrier.[52]

2.3. Steric Stabilization

Colloids can also be stabilized by the attachment of polymer chains or other linear molecules. The mechanism for this is entropic; when the colloids approach, the attached chains begin to interact in the space between the colloids. This interaction results in the reduction in the number of conformations available to the chains, thus lowering their entropy and so increasing the free energy of the system. This acts like a repulsive force and is known as steric stabilization.[45,48] This mechanism can be realized by attaching polymers to nanotubes either covalently or by physical adsorption. However, if the chains are physisorbed, they tend to be weakly bound and so are mobile and can even desorb. This makes modeling extremely complicated.

For covalently bound polymer chains, the repulsive potential has been calculated for both low and high polymer coverage.[45] In each case we can write

$$V(D) = B' e^{-D/L} \tag{12}$$

Where B' depends on the coverage of polymer chains (chains per unit area) and L is related to the thickness of the polymer layer. As before, the total potential is the sum of van der Waals and steric components and has a shape similar to that shown in Figure 1.

3. Dispersion and Exfoliation of Nanotubes in Solvents

In recent years a number of papers have appeared describing the preparation of stable suspensions of SWNTs in a range of common solvents.[16,17,21–23,53–55] In 1999 Liu et al. showed that individual SWNTs could be deposited from *N,N*-dimethylformamide (DMF) dispersions.[54] Shortly afterwards Ausman et al.[16] demonstrated dispersion of SWNTs in a number of solvents including *N*-methyl-2-pyrrolidone (NMP). The authors suggested that the criteria for a successful solvent were high electron pair donicity, low hydrogen bond donation parameter, and high solvatochromic parameter. Bahr et al. demonstrated metastable dispersion of SWNTs in a range of common solvents.[17] Furtado et al.[21] have shown that SWNTs can be debundled to a significant degree in both DMF and NMP. Landi et al.[22] followed this up with a quantitative study of SWNT dispersion in a range of amide solvents. In addition Maeda et al.[23] showed that SWNTs could be dispersed in mixtures of tetrahydrafuran with various amines. More recently, Detriche et al.[20] and Ham et al.[56] suggested that good solvents for nanotubes were determined by Hansen solubility parameters. One common factor in most of these papers is that NMP and DMF are widely considered to be the best nanotube solvents. In addition, it appears that the pool of other successful solvents is very small.

In this section, we will discuss the detailed characterization of dispersions of nanotubes in common solvents. We focus on the separation of an isotropic phase of dispersed nanotubes and the subsequent exfoliation which occurs as this phase is diluted. We will also discuss what makes a good solvent, specifically the various solubility parameters which have been used to describe nanotube–solvent mixtures.

3.1. Maximum Attainable Concentration

In general nanotubes are dispersed in solvents by sonication followed by mild centrifugation. The role of the sonication is to break up the highly aggregated nanotube powder into smaller aggregates such as bundles and to accelerate the exfoliation of individual nanotubes from the surface of these bundles.[57] Subsequent centrifugation removes any remaining aggregates, leaving a dispersion consisting of nanotubes and small bundles.[58,59] The concentration remaining after centrifugation (and so the quantity of aggregates removed) can be measured by absorption spectroscopy.[21,22,58,59] In all solvents, the fraction of aggregates removed tends to increase with increasing nanotube concentration from close to zero to 100% over a well-defined concentration range.[58–60] In our work on nanotubes dispersed in γ-butrylactone (GBL) before centrifugation, cross-polarized microscopy has revealed regions of aligned nanotubes which appear over the same concentration range as the aggregates.[58] This is reminiscent of the formation of a biphasic (isotropic and nematic) liquid crystal as predicted by Flory's theory.[61,62] Indeed, nematic nanotube phases have been produced and can be removed by centrifugation.[60] However, we must be careful before associating aligned aggregates in GBL or NMP with a nematic phase: The measured concentration where aligned aggregates begin to form in GBL is $C_1 \approx 0.01\ \mathrm{mg\,mL^{-1}}$. This is much lower than the value of $C_2 \approx 3.3\rho d/l \approx 15\ \mathrm{mg\,mL^{-1}}$ predicted theoretically for the onset of liquid crystallinity in athermal nanotube systems.[62] In addition, contrary to what would be expected for a liquid crystalline phase, the concentration after centrifugation also depends on the sonication conditions; optimization of sonication for nanotubes dispersed in cyclohexyl-pyrrolidone (CHP) has

reduced the aggregate content significantly.[63] Thus, the formation of aligned aggregates in solvent dispersion may not be linked to liquid crystal formation.

As mentioned above, aggregates can be removed by centrifugation and decantation of supernatant. Subsequently, for good solvents, one obtains a dispersion of small bundles and individual nanotubes.[21,58,59] The concentration achieved after centrifugation will be described in more detail in Section 3.2. Such centrifuged dispersions are very stable. Sedimentation measurements show no subsequent fall-out over periods of months.[18,58,59,63] In addition, we have measured the distribution of bundle diameters immediately after centrifugation and after some time for nanotubes dispersed in both *N*-methyl pyrrolidone[59] and γ-butrylactone.[58] In both cases no aggregation was observed confirming the stability. However, care must be taken with storage of these dispersions. Water uptake by the relatively hygroscopic NMP results in significant aggregation. We have found that addition of small quantities of water induce measureable aggregation. Addition of 10 wt% water results in a doubling of the typical bundle diameter and the removal of all individual nanotubes.[64]

3.2. Solubility Parameters

It has long been known that nanotubes can be dispersed in a number of solvents such as NMP, DMF, and so on. However, the question remains as to what determines which solvents actually disperse nanotubes. A related question is what determines the concentration remaining after centrifugation. As discussed in Section 2.1, molecular solutions are generally characterized by their intermolecular interactions and mixing thermodynamics. Within this framework, good solvents are those with the appropriate solubility parameters. To test whether this concept also applies to nanotubes, we measured the concentration of nanotubes remaining after centrifugation (for a given set of sonication/centrifugation conditions) in a wide range of 64 solvents.[19]

We found that the nanotubes concentration varied from $\sim$0 mg mL^{-1} for a number of solvents including THF to 3.4 mg mL^{-1} in cyclohexyl-pyrrolidone (CHP). In order to correlate the nanotube concentration with solvent properties, we have analyzed this data in terms of various solubility parameters.

Probably the simplest solubility parameter is the refractive index, as indicated by Equations 3 and 4. We note that this expression is appropriate for solute molecules that interact solely through dispersive forces. This is likely to be reasonably valid for carbon nanotubes. The nanotube concentration after centrifugation plotted as a function of solvent refractive index, n_B (589 nm), is plotted in Figure 2A. This data displays a sharp peak for solvents with $1.45 < n_B < 1.55$. Taking Equations 3 and 4 at face value, this suggests an average nanotube refractive index of $\sim$1.5. This is significantly lower than the value of $\sim$1.9 which can be estimated for (6,5) nanotubes from optical characterization of nanotube dispersions.[65]

However, the most commonly used solubility parameters are Hildebrand parameters. We have plotted the concentration after centrifugation versus the Hildebrand solubility parameter of the solvent, as shown in Figure 2B. This gave a clear peak for solvents with $\delta_T \approx 23$ MPa$^{1/2}$. This suggests that nanotubes can be treated as a molecule with Hildebrand parameter close to 23 MPa$^{1/2}$, in line with measurements by Detriche et al.[20] and Ham et al.[56] However, the peak was not very well defined, as many solvents with δ_T close to the peak displayed lower than expected nanotube concentrations. This suggests that δ_T alone is insufficient to describe good solvents. In general, under such circumstances, Hansen solubility parameters are required. To test this, we plotted the nanotubes concentration versus δ_D, δ_P, and δ_H individually. We found a well-defined peak in the *C* versus δ_D graph centered at $\sim$18 MPa$^{1/2}$ and with width $\sim$2.5 MPa$^{1/2}$. Broader peaks were found in the *C*versus δ_P and δ_H graphs. In each case the peaks were centered at $\sim$7.5 MPa$^{1/2}$ and had widths of $\sim$7 MPa$^{1/2}$. This is interesting and unexpected; due to their non-polar nature it had been expected that non-polar solvents would best disperse nanotubes. However, this work clearly shows that non-zero values of polar and H-bonding solubility parameters are required.

However, nanotubes differ from normal molecules in that they possess a well-defined surface. This suggests that traditional solubility parameters may be inappropriate. With this in mind, we derived an approximate expression, based on surface localized

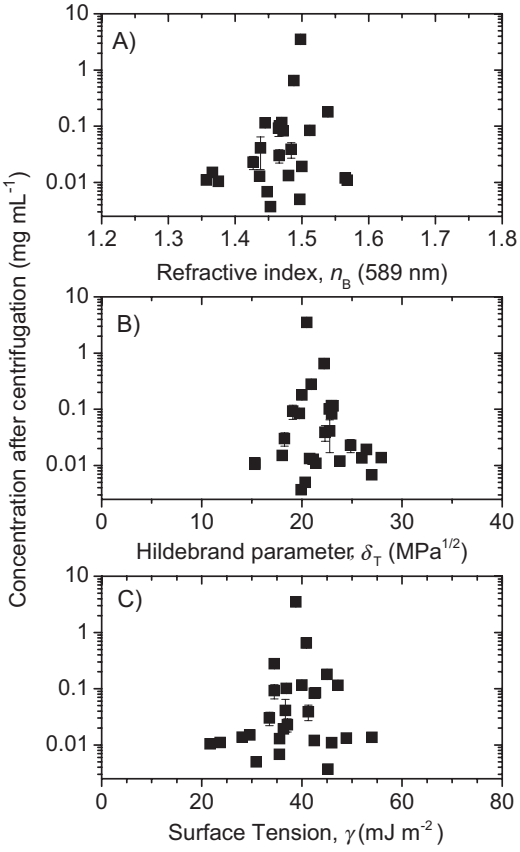

Figure 2. Nanotube concentration after centrifugation, C_{Max}, for a range of solvents as a function of A) solvent refractive index, B) solvent Hildebrand parameter, and C) solvent surface tension. Reproduced, in part, with permission from Ref. [19]. Copyright 2009 American Chemical Society.

van der Waals type interactions, for the enthalpy of mixing (per solvent volume), $\Delta\overline{H}_{mix}$, when nanotubes are dispersed in a solvent:[18]

$$\Delta\overline{H}_{mix} \approx \frac{2}{R_{bun}}(\delta_{NT} - \delta_{sol})^2\phi \quad (13)$$

where R_{bun} is the radius of the dispersed nanotubes bundles and ϕ is the nanotube volume fraction. Here δ_{NT} and δ_{sol} are the square roots of the nanotubes and solvent surface energies. We note that this equation is very similar in form to Equation 7. These parameters can be thought of as new solubility parameters. This expression predicts that good solvents are those with surface energies close to the nanotube surface energy. Plotting the nanotube concentration versus the solvent surface tension, as shown in Figure 2C, we found a well-defined peak for surface tension close to 40 mJ m^{-2}.[18,19] This corresponds to a surface energy of 70 mJ m^{-2}, well within the range of surface energies measured for nanotubes and graphite. While the knowledge that good solvents have surface tensions close to 40 mJ m^{-2} has proved useful for solvent identification, it is not a perfect criterion. It is likely that, as with Hansen parameters, good solvents must have the correct balance of dispersive, polar, and H-bonding components[66,67] of surface energy.[19] In addition, reduced configurational entropy associated with π stacking of solvent molecules at the nanotubes surface may prohibit nanotubes dispersion in otherwise promising solvents.[68]

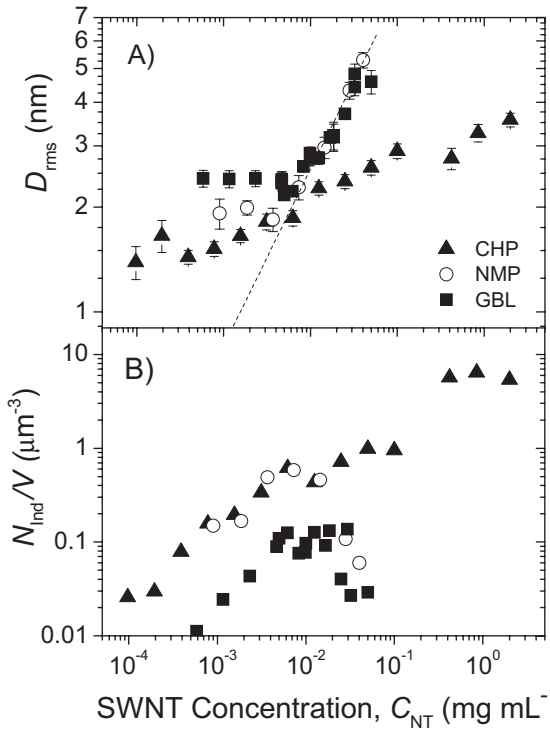

Figure 3. Quality of nanotube dispersion in the solvents CHP, GBL, and NMP as a function of nanotube concentration. A) Root mean square SWNT bundle diameter, as garnered from AFM statistics. B) Number of individual nanotubes per unit volume of solvent. Adapted from Refs. [58, 59].

3.3. Nanotube Exfoliation

Critically important is the dispersion quality in these post-centrifugation dispersions. In the ideal case, one would have dispersions of completely individualized nanotubes. However, this is rarely achieved; even in ultra-centrifuged, surfactant- or DNA-stabilized dispersions, significant quantities of bundles are present.[38,69–71] We have characterized the exfoliation state of solvent-dispersed tubes by depositing them on substrates (mica, SiO_2, or HOPG) and performing atomic force microscopy (AFM) to measure the bundle diameter distribution. We performed a number of checks to confirm that these distributions represented the properties of the dispersion rather than the effects of aggregation on deposition.[59,72,73] We have found that, after centrifugation, for all solvents investigated, the bundle diameter ranges from 1 nm (individual SWNTs) to ~10 nm with a root mean square (rms) diameter of $D_{rms} \approx 5$–6 nm. As is common for DNA- and surfactant-stabilized dispersions, this diameter distribution can be substantially improved by removing most of the bundles by ultracentrifugation.[74] However, this process is wasteful, especially considering that good-quality SWNTs cost between $500 and $1 500 per gram. Seeking an alternative route to improve the dispersion quality, we were inspired by the Gibbs–Duhem theorem,[47] which lead us to reason that removing solute mass (centrifugation) and addition of solvent volume (dilution) should give equivalent results. While this is not rigorous (nanotube–solvent mixtures may not be true solutions), we nevertheless tested the effect of dilution (addition of solvent) on the bundle diameter distribution.

For every solvent tested we have observed an improvement in dispersion quality on dilution. This is manifested by a decrease in rms bundle diameter with decreasing concentration (the bundle length tends to remain constant). This is illustrated in Figure 3 for nanotubes dispersed in the solvents NMP, CHP, and GBL. In addition, empirically the rms bundle diameter generally scales well with $\sqrt{C_{NT}}$ (dashed line) before saturating at $D_{rms} \approx 2$ nm at low concentrations. We can rationalize this $\sqrt{C_{NT}}$ behavior by noting that the hypothesis of a constant bundle number density, $(N/V)_{Eq}$, results in the prediction for such scaling:[59]

$$D_{rms} = \sqrt{\langle D^2 \rangle} \approx \left[\frac{4C_{NT}}{\rho_{NT}\pi L_{bun}(N/V)_{Eq}}\right]^{1/2} \quad (14)$$

where ρ_{NT} is the nanotube density, L_{bun} is the bundle length, and $(N/V)_{Eq}$ is the equilibrium bundle number density. A noteworthy exception to this rule is CHP, which has a much weaker dependence of D_{rms} on C_{NT}. We note that CHP is distinctive as it displays by far the highest levels of nanotube dispersibility.

Another interesting observation is that $(N/V)_{Eq}$ is set by the nanotube length. For NMP at least, $(N/V)_{Eq}$ is very close to the number density defined by one bundle occupying, on average, the spherical volume whose diameter is equal to the bundle length.

As the concentration is increased, the bundle diameters increase but $(N/V)_{Eq}$ remains constant.[59]

Once the diameter distribution is known, we can measure the fraction of individual nanotubes, N_{Ind}/N_T. In all cases, this tends to increase as the concentration is decreased,[58,59,63] reaching ~80% for nanotubes in CHP at $C_{NT} < 10^{-3}$ mg mL^{-1}.[63] One can also calculate the number of individual nanotubes per unit volume from

$$\frac{N_{Ind}}{V} = \frac{N_{Ind}}{N_T}\frac{4C_{NT}}{\rho_{NT}\pi\langle D^2\rangle\langle L\rangle} \quad (15)$$

For most solvents, N_{Ind}/V increases with increasing concentration before peaking and falling off at higher concentrations as high-concentration aggregation begins to dominate.[58,59,63] This behavior is shown in Figure 3B for NMP-, GBL-, and CHP-based dispersions. Interestingly, even though the D_{rms} versus C_{NT} data are very similar for NMP and GBL, these solvents display different N_{Ind}/V behavior. This suggests the shape of the diameter distribution is strongly solvent dependent. We note that for NMP-based dispersions, we could confirm the AFM results by measuring the photoluminescence (PL) intensity as a function of concentration. As PL is only observed for individual nanotubes, its intensity should scale with N_{Ind}/V. Very good proportionality was observed between the PL intensity and N_{Ind}/V, confirming the validity of the AFM results[18,59] (note that this test is not straightforward, as PL is significantly quenched in all good solvents, making quantitative measurements difficult). Once again CHP is the exception with N_{Ind}/V increasing over the entire concentration range. We again note that nanotube/CHP dispersions have far better dispersibility than any other solvent. This is probably because CHP has solubility parameters very close to those of nanotubes,[19] making it a virtually ideal solvent.

3.4. Spontaneous Exfoliation and Solubility

It is important to consider the question as to whether nanotubes can be thermodynamically soluble in any solvents. Due to their size and rigidity, their entropy of mixing would be small.[19] This means that, to display a negative free energy of mixing, the nanotube–solvent interaction would have to be such that the enthalpy of mixing was very small or negative. We speculated that this may indeed be the case for solvents with just the right surface energy. Indeed, the presence of an equilibrium bundle number density[59] suggests the presence of an adsorption/desorption equilibrium for nanotubes and bundles. This would require the ability for nanotubes to spontaneously desorb from bundles, which suggests solubility. Indeed we observed that when a nanotube dispersion in NMP is diluted without sonication, a significant reduction in bundle size with time is observed, consistent with spontaneous exfoliation.[18] To test this we used light scattering to measure the Flory–Huggins parameter (and so the enthalpy of mixing) of SWNT–NMP dispersions. This gave a value of $\chi = -0.074$, very slightly negative. This suggests that nanotubes are actually thermodynamically soluble in NMP. Unpublished results by Prof James Hamilton and co-workers (University of Wisconsin, Platteville) show negative χ values for some other solvents, notably CHP. However, we note that some bundles are always observed in solvent dispersions. This should not be the case for a true solution.[45] In addition, analysis of the data in Section 3.2 with Flory's rigid-rod theory would suggest that χ cannot be negative.[19] Thus, the question of solubility and indeed the exact mechanism for nanotube dispersion and exfoliation in solvents remains unclear.

4. Surfactant Stabilization of Nanotubes

Early on in nanotube research, it became clear that it would be advantageous to disperse and exfoliate nanotubes in the liquid phase. Back then, it was widely believed that their size and rigidly ruled out standard dissolution in solvents. As a result, researchers began to treat nanotubes as colloids, allowing the use of a wide range of stabilization and processing techniques used in colloid science.[50] The simplest and most common colloidal stabilization technique applied to nanotubes was the use of surfactants as an interfacial stabilizer to aid their dispersion in water.

The earliest examples of this work date from 1997–8 with the demonstration of stable dispersions of surfactant-coated nanotubes and small bundles.[33,75–78] However, this stabilization technique really took off in 2000 with the observation of fluorescence in surfactant-stabilized nanotube dispersions[34] and the demonstration that similar dispersions could be used to prepare strong fibers.[79] Since then, thousands of papers have been published describing work which relies on surfactant-stabilized nanotubes. In addition, a number of reviews have appeared.[31,80]

While nanotubes can be dispersed using many surfactants,[81] the most common ones used in nanotube research are probably sodium dodecyl sulphate (SDS), sodium dodecylbenzene sulphonate (SDBS), and sodium cholate (SC). There are a number of advantages gained by using surfactants to disperse nanotubes. Nanotubes can be dispersed at reasonably high concentrations, reportedly up to 20 mg mL^{-1}.[82] In addition, nanotubes tend to be highly exfoliated; large quantities of individual nanotubes are observed by atomic force microscopy[82] and photoluminescence spectroscopy.[83,84] That the nanotubes electronic properties are minimally perturbed by the (van der Waals) interaction with the surfactant allows the basic characterization of the nanotubes. Finally, the fact that the solvent used is invariably water is an important advantage for environmental and safety reasons. However, surfactants are not without their disadvantages; in many cases they must be removed after processing. For example, although thin transparent films have successfully been produced from surfactant/nanotube dispersions,[85,86] post treatment with acids is required to remove residual surfactant.[87]

In this section, we focus on the observation that the exfoliation state of nanotubes/surfactant dispersions scales with concentration. We use this to develop metrics to describe the quality of the dispersion. These metrics are shown to depend on the zeta potential of the nanotube dispersion. Finally we compare dispersion quality for diluted dispersions to that measured for ultracentrifuged dispersions.

4.1. Concentration Dependence

As described in Section 3.3, an important property of nanotube/solvent dispersions is that the dispersion quality improves as the

nanotube concentration is decreased. This is manifested by a decrease in rms bundle diameter coupled with an increase in the fraction of individual nanotubes with decreasing concentration. As surfactant stabilization of nanotubes is probably the prevalent dispersion technique, we considered whether concentration dependent exfoliation might occur in such systems. To test this we prepared a stock dispersion of surfactant-stabilized nanotubes by adding nanotubes ($C_{NT} = 1\,mg\,mL^{-1}$) to an aqueous SDBS solution ($C_{SDBS} = 5\,mg\,mL^{-1}$).[88] This was then mildly centrifuged to give a dispersion with $C_{NT} = 0.28\,mg\,mL^{-1}$. We note that the surfactant concentration generally needs to be above the critical micelle concentration (CMC, $\sim 0.7\,mg\,mL^{-1}$ for SDBS)[52,89] and the surfactant concentration needs to substantially exceed the nanotube concentration[79,82,88] to achieve stable dispersions. This stock solution was then diluted to varying degrees by mixing with an aqueous SDBS solution ($C_{SDBS} = 5\,mg\,mL^{-1}$) to create a dilution series, sonicating after every dilution. In all cases the bundle diameter and length distributions were measured by AFM and statistical analysis carried out.

The rms bundle diameter for nanotubes stabilized with SDBS decreased with the square root of the nanotube concentration before saturating at ~2 nm at low concentration (see Fig. 4).[88] This behavior is very similar to that displayed by a number of solvents including NMP. The main differences are that higher nanotube concentrations are achieved using surfactants compared to all solvents (except CHP) and that the D_{rms} versus C_{NT} curve for the surfactant dispersions was shifted to higher concentrations (by a factor of ~7 compared to NMP). This means that bundles of a given diameter can be achieved at concentrations 7 times higher for nanotubes in SDBS/water compared to NMP. In addition, the maximum number of bundles and nanotubes achievable (N_{Tot}/V) in the SDBS dispersion was close to $10\,\mu m^{-3}$ compared to $< 1\,\mu m^{-3}$ in most solvents (with the exception of CHP). In addition, the population of individual nanotubes was much higher in SDBS than in NMP over almost the entire concentration range studied. This was most obviously manifested in measurements of the fraction of individual nanotubes, N_{Ind}/N_T, and the number of individual nanotubes per unit volume of solution, N_{Ind}/V. We attempted to confirm the concentration scaling of N_{Ind}/V by measuring the nanotube PL intensity. However, at the higher concentrations associated with the SDBS-stabilized samples, inner filter and re-absorption[90] effects became problematic. However, the PL data qualitatively supported the AFM data.

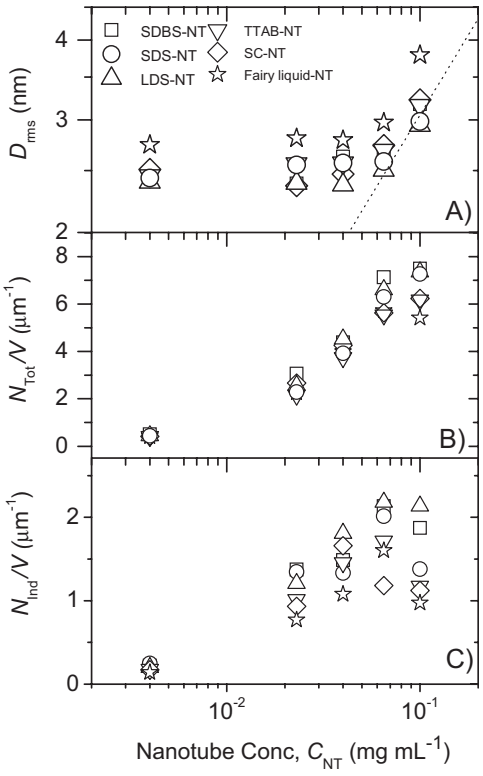

Figure 4. A) Root mean square bundle diameters for SWNTs dispersed in different surfactants as a function of concentration obtained from AFM measurements. The dash–dot line illustrates $D_{rms} \propto \sqrt{C_{NT}}$ behavior as observed in many systems. B) Total number density of bundles/individuals versus concentration for SWNTs dispersed in different surfactants. C) Number of individual nanotubes per unit volume for SWNTs dispersed in different surfactants. Reproduced with permission from Ref. [52]. Copyright 2008 American Chemical Society.

4.2. Importance of Zeta Potential

The reason dispersion quality in SDBS-based dispersions is much higher than for most solvent–nanotube dispersions is due to Coulomb repulsion between nearby surfactant-coated nanotubes (see Section 2.2). This repulsion means that in surfactant-stabilized dispersions, nanotubes can exist in close proximity to each other without the possibility of aggregation, resulting in high-quality dispersions.

It is possible to quantify the degree of Coulomb repulsion via the zeta potential. As discussed in Section 2.2, this is the electric potential at the edge of the bound surfactant tail groups and is proportional to the effective charge on the coated nanotube.[91] If Coulomb repulsion is important for surfactant-stabilized nanotube dispersions, then the dispersion quality would be expected to scale with the zeta potential.

To test this, we first need quantifiable metrics for the dispersion quality. We adapted these metrics from the concentration dependent work described in Sections 3.3 and 4.1. We proposed that the quality of the dispersion could be measured by the saturation values of D_{rms} at low concentration, the saturation value of N_{Tot}/V at high concentration and the maximum value of N_{Ind}/V (generally obtained at intermediate concentration). Once the metrics were defined we needed to measure them for nanotubes dispersed in a range of surfactants. We measured the bundle diameter distribution as a function of concentration for nanotubes dispersed using SDBS, SDS, SC, lithium dodecyl sulfate (LDS), tetradecyl trimethyl ammonium bromide (TTAB), and Fairy liquid (FL, a commercial dishwashing liquid).[52] From these diameter distributions, we measured the metrics described above. Figure 4 illustrates the concentration dependence of D_{rms}, N_{Tot}/V, and N_{Ind}/V. In addition, for each dispersion we measured the zeta potential at the concentration appropriate for each metric. We found that for N_{Tot}/V and N_{Ind}/V, each dispersion quality metric increased linearly with the zeta potential (Fig. 5). In addition we found that D_{rms} decreased as zeta increased. This is exactly the

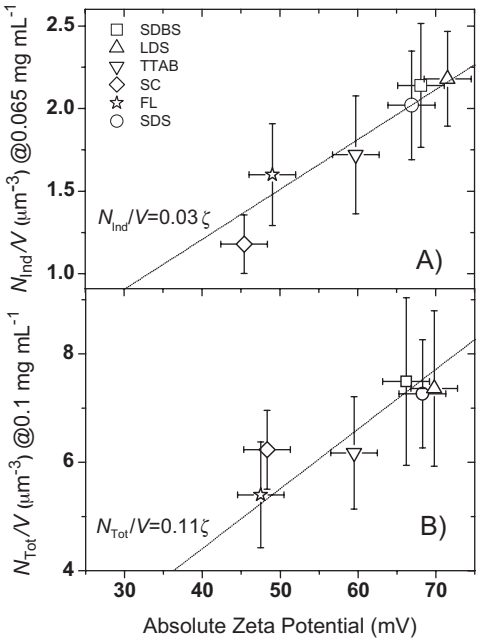

Figure 5. Scaling of dispersion quality metrics versus absolute mean zeta potential of nanotubes dispersed using each surfactant type. In each case the metric is measured at a particular nanotube concentration which is indicated by the labeling scheme: metric@concentration. A) N_{Ind}/V @ 0.065 mg mL^{-1} versus $|\bar{\zeta}|$. B) N_{Tot}/V @ 0.1 mg mL^{-1} versus $|\bar{\zeta}|$. In (A) and (B), the dashed line illustrates linear scaling. Note that the errors in this figure were calculated by considering the standard error of the distribution of D^2. Reproduced with permission from Ref. [52]. Copyright 2008 American Chemical Society.

behavior expected and confirmed that the dispersion quality and the nanotube exfoliation state depends critically on the Coulomb repulsion between surfactant-coated nanotubes. We have also found that the zeta potential increases with decreasing surfactant size. This allows is to predict that low molecular weight surfactants that pack tightly on the nanotube surface are ideal.[52]

4.3. Dilution versus Ultracentrifugation

While we have shown that dispersion quality can be enhanced by dilution, we have not commented on how the dispersion quality compares to dispersions where bundles are removed by ultracentrifugation, the most common technique.[34,92] To test this we prepared a stock SDBS/nanotube dispersion which we split in two, ultracentrifuging one half.[69] The other half was then diluted to match the concentration of the ultracentrifuged portion. These two dispersions were then characterized by AFM as well as absorption and fluorescence spectroscopy. We found that the ultracentrifuged sample had four times as many individual nanotubes as the diluted sample when compared at a given concentration. However, ultracentrifugation also resulted in eight times as much nanotube wastage (mass loss on ultracentrifugation). It appears that both techniques have advantages which may be important depending on the circumstance.

5. Biomolecules

In addition to surfactants, nanotubes can be stabilized in water by coating with other molecules, notably polymers[30,93] and biomolecules such as DNA.[94–98] SWNTs have been dispersed in water using both natural DNA[94–96] and short, custom-synthesized oligonucleotides.[97,98] These dispersions have the advantage of using water as the solvent, which is very safe, readily available, and necessary for any potential medical or biological applications. The DNA bonds non-covalently to the nanotube which preserves the nanotubes' electrical and optical properties.[99,100] In addition, DNA-dispersed SWNTs can be separated by diameter using ion-exchange chromatography[97,98] or by ultracentrifugation through an aqueous density gradient.[101] Additionally, if one chooses, oligonucleotides can be removed using small aromatic molecules such as rhodamine 6G or the complementary DNA strand, once any necessary processing is complete.[99] A variety of different applications, such as fiber spinning,[102] self-assembled nanotube field-effect transistors,[103] stabilization of colloidal particles,[104] chemical sensing,[105] and both medical diagnostic and biological fields[100,106–109] have been investigated for DNA-dispersed SWNTs.

In general, the stabilization mechanism for DNA-coated nanotubes is similar to that for surfactant-coated nanotubes. The DNA backbone carries a charge which is balanced by a cloud of counter-ions. Thus, DNA-coated nanotubes have a well-defined zeta potential. However, in the early stages of DNA wrapping, sections of the DNA probably extend into the solvent.[110] In this case, there may be a steric component to the stabilization.

The vast majority of published literature involves the dispersion of nanotubes with synthetic oligio-DNA or single-stranded DNA. In this section we characterize the dispersion of nanotubes using genomic (salmon sperm) double-stranded DNA. For comparison we also characterize dispersions prepared with a synthetic designed peptide. For the double-stranded DNA we also characterize the nature of the DNA wrapping around the nanotubes.

5.1. Dispersion in DNA and Peptides

We have prepared dispersions of nanotubes in both genomic, double stranded DNA[70] and using the designed peptide[111] (Nano-1). In each case we have prepared a range of samples with different nanotube concentrations. All samples were characterized by photoluminescence spectroscopy and, after deposition on a mica substrate, by AFM. For both DNA- and peptide-based dispersions we observed the bundle diameter to fall with decreasing concentration. However in neither case was $\sqrt{C_{NT}}$ behavior observed. In both cases the fraction of individual nanotubes increased with decreasing concentrations, with N_{Ind}/V displayed a peak at intermediate concentrations for the DNA-based sample. In the peptide samples N_{Ind}/V increased over the entire concentration range. We attempted to confirm the AFM results using PL measurements. However, no PL was observed for either sample. Surprisingly, intense PL was observed in the DNA sample one month later. Subsequently, the PL intensity for the different concentrations matched very well to the N_{Ind}/V data, thus supporting the AFM.

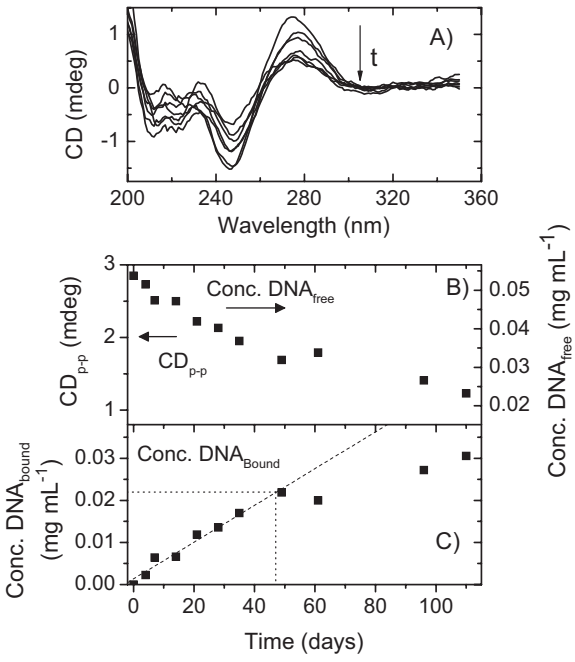

Figure 6. A) Circular dichroism spectra recorded at different times over a three-month period. The magnitude of the spectra was found to decrease continuously over the duration of the experiment. B) The CD peak to peak height (left axis) and the calculated concentration of free DNA (left axis) are shown as a function of time. C) The concentration of bound DNA is shown as a function of time. The dotted line shows the time at which a full monolayer coats the SWNT. The concentration of bound DNA was found to increase linearly up to this time and sublinearly thereafter. Reproduced with permission from Ref. [110]. Copyright 2008 American Chemical Society.

5.2. Evolution of Wrapping

To investigate the appearance of PL one month after preparation of the DNA/nanotube dispersions, we investigated the PL intensity as a function of time.[110] Initially zero, the PL intensity began to increase after 20 days, saturating after 50 days, having increased by a factor of 50. This increase is accompanied by a considerable sharpening of the nanotube absorption peaks. In addition, circular dichroism studies show the gradual denaturing of the DNA over the first 50 days (Fig. 6). High-resolution transmission electron microscopy (HRTEM) shows the denatured DNA forming a coating of DNA on the walls of the nanotube over a three-month period. After about 30 days, HRTEM images (Fig. 7) clearly show the DNA wrapping helically around the SWNTs in a surprisingly ordered fashion as predicted by modeling.[112] We suggest that the initial quenching of NIR photoluminescence and broadening of absorption peaks is related to the presence of protonated surface oxides on the nanotubes.[113,114] The presence of an ordered DNA coating on the nanotube walls mediates both the removal and the deprotonation of the surface oxides, resulting in the switching on of the PL. This work clearly shows that DNA coats nanotubes in a very ordered fashion. However, because this ordering means a decrease in entropy, it is a very slow process.

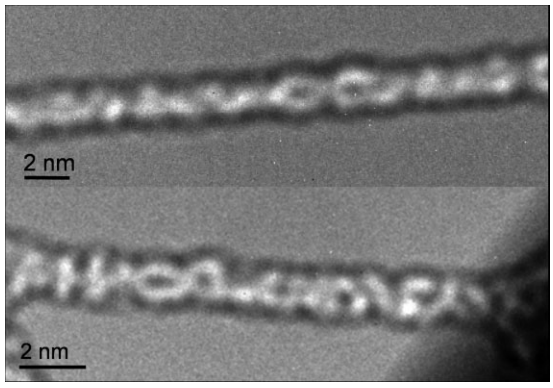

Figure 7. HRTEM images showing ordered DNA wrapping of nanotubes in a 32-day-old sample. Reproduced with permission from Ref. [110]. Copyright 2008 American Chemical Society.

6. Functionalization

Another strategy for nanotube dispersion, described in a wide range of papers and reviews,[24,115,116] is to covalently functionalize the nanotubes with bulky molecules. The functionalized nanotubes tend to form a (meta)stable colloidal suspension, sterically stabilized by the osmotic pressure induced when functional groups from adjacent nanotubes move into the same region of space (Section 2.3).[117] Additionally, in some cases stabilization is achieved by electrostatic interactions between the functional groups.[35] Furthermore, the functional group–solvent interaction lowers the enthalpy of mixing and can increase the entropy of mixing (solvent configurational effects) resulting in a lower free energy of mixing. In some cases the free energy of mixing may even be negative, resulting in a true solution.[118]

In this section we study the exfoliation state of covalently functionalized nanotubes. In addition, we explore the interaction between the functional groups and the solvent.

6.1. Interaction with Solvent

One advantage of functionalized nanotubes is that they can be dispersed in any solvent just by appropriate choice of functional group. This strongly suggests that the interaction with the solvent is controlled by the functional group rather than the chemical properties of the nanotube surface. To test this, we prepared dispersions from octadecylamine-functionalized nanotubes in a range of solvents.[119] The dispersions were centrifuged and absorption spectroscopy used to measure the concentration of nanotubes remaining. We plotted the concentration remaining versus the Hildebrand parameter of the solvent. As shown in Figure 8, this data showed a very well defined peak at $\delta_T = 19.5\,MPa^{1/2}$. This is exactly the value of the Hildebrand parameter of octadecylamine. This confirms that the solvent-functionalized nanotube interaction is completely controlled by the functional group.

6.2. Concentration Dependence

AFM was used to measure the bundle diameter distribution as a function of concentration for octadecylamine-, poly

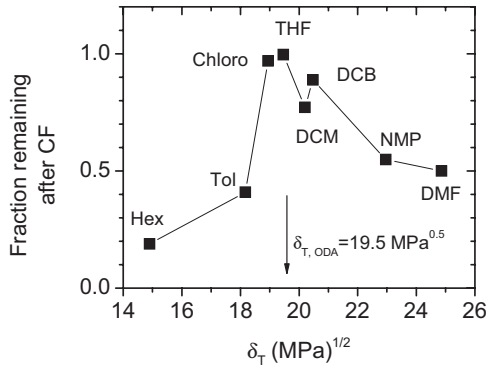

Figure 8. Fraction of SWNT–octadecylamine remaining after centrifugation versus solvent Hildebrand parameter. The Hildebrand parameter of octadecylamine is shown by the arrow. Reproduced with permission from Ref. [119]. Copyright 2008 American Chemical Society.

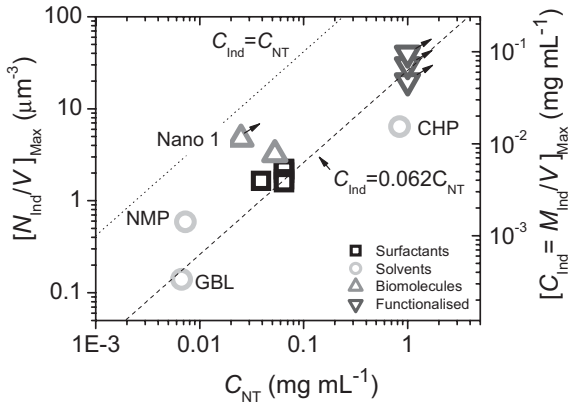

Figure 9. Comparison of the maximum measured population of individual nanotubes (N_{Ind}/V) as a function of the concentration where the maximum was observed for all dispersants discussed in this work. The right axis is transformed into the mass of individual nanotubes per unit volume, which is equivalent to the partial concentration of individual nanotubes. The arrows indicate the samples for which N_{Ind}/V had not peaked in the measured concentration range. The dotted line represents the situation where all nanotubes are perfectly exfoliated. The dashed line is a linear fit to all the samples studied.

(*m*-aminobenzene sulfonic acid)-, and poly(ethyleneglycol)- functionalized nanotubes.[119] In each case we found that the individualized nanotubes had diameters of ~3 nm. This diameter reflects the 1-nm diameter nanotubes and a 1-nm-thick shell of functional groups. At low concentration (~10^{-4} mg mL^{-1}) we observed rms bundle diameters of ~3–4 nm, indicative of extensive exfoliation. As the concentration was increased to 1 mg mL^{-1}, the rms diameter increased only to 5–6 nm. This represents a very small degree of aggregation over 4 decades of concentration change, illustrating the very good quality and stability of these dispersions. This was even more apparent when we plotted N_{Ind}/V as a function of nanotube concentration. Here we found that N_{Ind}/V increased monotonically with nanotube concentration over the whole concentration range, right up to 1 mg mL^{-1}. In fact, even at 1 mg mL^{-1}, while N_{Ind}/V displayed very high values of ~40 μm^{-3}, it had not yet peaked (although it had begun to turn over). This is in marked contrast to the vast majority of other systems, which show a well-defined maximum value of N_{Ind}/V at some concentration well below 1 mg mL^{-1}. This behavior illustrates that functionalization is undoubtedly the best route to achieve high degrees of exfoliation at high concentrations.

7. Comparison of Nanotube Dispersants

In this review we have studied fourteen different dispersions divided into four distinct dispersant types: solvents, surfactants, biomolecules, and functional groups. In all cases we have quantified the dispersion quality using a number of well defined metrics. This gives us the ability to compare dispersion quality for the four dispersant types.

Before doing this, it is worth considering what the ideal scenario would be. The ideal dispersant would exfoliate nanotubes such that all nanotubes were exfoliated even at the highest concentrations. This is clearly unattainable. The best we can hope for is to maximize the fraction of individual nanotubes at as high a concentration as possible. As discussed above, the fraction of individual nanotubes tends to decrease with increasing concentration.[58,59,63,69,88,111,119] Thus, this is a poor metric as it ignores the requirement that it be large *and* the total concentration be high. A better metric is the number of individual nanotubes per volume, N_{Ind}/V. This quantity generally displays a peak when plotted versus concentration,[58,59,63,69,88,111,119] simply because at low concentration there is not much nanotube material, but a large fraction of it is individualized, while at high concentration the opposite holds true. Thus for a good dispersant we would expect the peak value of N_{Ind}/V to be high *and* the peak to occur at a high concentration.

We measured the peak value of N_{Ind}/V and the concentration at which it peaked for all samples discussed in this review. This data is plotted in Figure 9. To simplify the interpretation, we have multiplied the left axis by the average nanotube mass (calculated for 1-μm-long, 1-nm-diameter nanotubes) to show the total mass of individual nanotubes per volume on the right axis. This is equivalent to the partial concentration of individual nanotubes.

From this graph we can clearly state that biomolecules and surfactants are similar in their ability to exfoliate nanotubes. In both cases, they can disperse individual nanotubes at 0.5–1 × 10^{-2} mg mL^{-1} for a total concentration of 2–7 × 10^{-2} mg mL^{-1}. Also, it is very clear that the functionalized nanotubes are by far the best performers with partial concentrations of individual nanotubes approaching maximum values of ~0.1 mg mL^{-1} for total concentrations of 1 mg mL^{-1}. We note that the data for the surfactants, biomolecules, and functionalized samples tends to clump together by type. However the solvent data is quite spread out. GBL, which we would class as a medium-quality solvent, is at the bottom left of the graph, NMP, which we consider a good solvent, is a bit higher up while CHP, which we consider an excellent solvent, approaches the functionalized data. Clearly, the range of behavior displayed by solvents is much broader than that for the other dispersants. This is consistent with the fact that the solvent–nanotube can be tuned over a very wide range, simply by appropriate choice of solvent solubility parameters.

Interestingly, $[N_{Ind}/V]_{Max}$ (a.k.a. $[C_{Ind}]_{Max}$) scales approximately linearly with $[C_{NT}]_{Max}$ for all four dispersant types (dashed line). The dashed trend line is described by $[C_{Ind}]_{Max} = 0.06[C_{NT}]_{Max}$. This means that for all dispersants, the sample with the peak population of individual nanotubes consists of ~6 wt% individuals. This is a rather surprising result and may reflect universal effects associated with exfoliation at high concentrations. An exception was the synthetic peptide Nano-1, which displayed $[N_{Ind}/V]_{Max}$ values significantly closer to the theoretical maximum value illustrated by the dotted line (all nanotubes exfoliated).

This comparison clearly shows that if large populations of nanotubes are required at high concentrations, then nanotube functionalization is clearly the answer. However, if one wants to avoid the irreversible damaging associated with functionalization, then dispersion in CHP may be appropriate. If on the other hand, one requires aqueous systems, then both surfactants and biomolecules perform reasonably well.

8. Exfoliation of Graphene

Graphene is a two-dimensional carbon crystal and is closely related to nanotubes. The unprecedented mechanical,[120] electrical,[121] and thermal properties[122] of graphene have sparked huge interest among researchers in recent years.[3] While many of the groundbreaking experiments have been carried out on micromechanically cleaved monolayers,[123] future industrial applications are likely to require large-scale, high-throughput processing methods.[124] Early progress in this area involved the oxidization of graphite, followed by exfoliation in water, to give aqueous dispersions of graphene oxide (GO).[125,126] This material consists of sp^2-bonded carbon sheets decorated with large numbers of covalently bonded hydroxyl and epoxide groups. The polar nature of these groups, coupled with the Coulomb repulsion associated with extensive proton dissociation,[127] means that these dispersed GO sheets are very stable in aqueous environments. Such dispersions are very useful as they facilitate both materials processing and fundamental characterization.

However, GO faces some significant disadvantages. Due to the disruption in the π-orbital structure on oxidization, GO is a poor electrical conductor.[128] The oxides can only be removed by thermal or chemical reduction. However, reduction cannot remove the many structural defects introduced by the oxidation process.[128–133] These defects disrupt the band structure and completely degrade the electronic properties which make graphene unique.

To combat these problems, a simple, large-scale, high-yield method is required to exfoliate graphite to give graphene with the introduction of defects or oxides. In this section we describe two methods to do this; solvent-assisted and surfactant-assisted exfoliation.

8.1. Solvents

In Section 3.2 we discussed how matching of nanotube and solvent surface energies is one criterion for a successful nanotube solvent. However, the surface energies of nanotubes and graphene are expected to be similar. This suggests that it may be possible to exfoliate graphite to give graphene in NMP in the same way nanotubes can be exfoliated. To test this, we sonicated graphite powder in NMP followed by mild centrifugation.[41] We note that both sonication and centrifugation regimes are much milder for graphite than for carbon nanotubes. This resulted in pale gray dispersions (Fig. 10A). Absorption spectroscopy showed the concentration of graphitic material remaining after centrifugation to be ~0.01 mg mL^{-1} in a number of solvents (Fig. 10B). In order to characterize the exfoliation state of the dispersed graphitic material, we deposited a small quantity into a TEM grid for microscopic analysis. On the grid we observed large quantities of two-dimensional flakes with lateral dimensions from ~500 nm to ~3 000 nm. In many cases, these flakes had straight edges and corners with well defined angles, typically 60°, 90°, or 120°. In many cases it was clear that the flakes consisted of a well-defined number of layers and, in most cases, careful examination of the edges allowed the estimation of the number of layers. In approximately 30% of cases, the flakes consisted of one layer; monolayer graphene (Fig. 11). That these were definitely graphene monolayers could be confirmed by electron diffraction through the difference in intensity of {2110} and {1100} diffraction spots.[134]

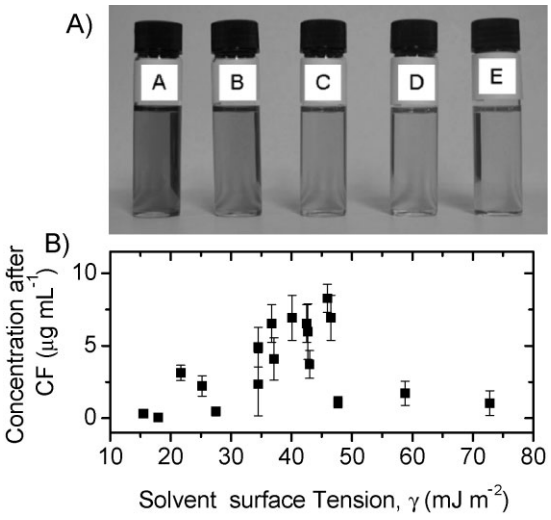

Figure 10. A) Dispersions of graphene in NMP, at a range of concentrations ranging from 6–4 μg mL^{-1} (A–E) after centrifugation. B) Graphene concentration measured after centrifugation for a range of solvents plotted versus solvent surface tension. Reproduced from Ref. [41].

Such dispersion and exfoliation was observed in a range of solvents. In addition, as shown in Figure 10B, the concentration of dispersed material (after centrifugation) showed a peak for surface tensions close to 40 mJ m^{-2}. This is exactly the same behavior observed for nanotubes dispersed in solvents and confirms that the solvent–graphene interaction is van der Waals rather than chemical.

We also checked that the exfoliation procedure was non-destructive and did not introduce oxides or structural defects. X-ray photoelectron spectroscopy carried out on vacuum-filtered films showed a carbon 1s peak virtually identical to HOPG. No evidence of oxides was observed. In addition, Raman spectroscopy showed no significant increase in D-band intensity confirming that the processing had not introduced structural defects.

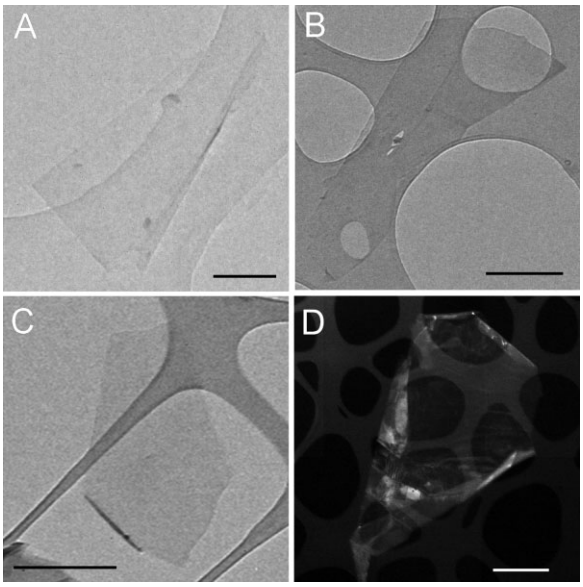

Figure 11. A–C) Bright field TEM images of single-layer graphene flakes deposited from γ-butrylactone, dimethyl-imidazolidinone, and *N*-methyl-pyrrolidone respectively (scale: 500 nm). D) Dark-field TEM of a graphene layer showing extensive scrolling at the edges (scale: 1 μm). Reproduced from Ref. [41].

However, the maximum concentration achieved ($\sim$0.01 mg mL^{-1}) is too low to be useful in many applications. In order to increase this concentration we employed a low-power sonication regime over long time frames.[135] We added graphite powder to 1 L of NMP (3 mg mL^{-1}) in a round bottomed flask. This was sonicated continuously in a low power sonic bath for $\sim$460 hours. Periodically, small aliquots were removed and centrifuged. The concentration in each of these aliquots was measured using absorption spectroscopy and a drop deposited on a TEM grid. We found that the concentration remaining after centrifugation increased to $\sim$2 mg mL^{-1} after 460 hours. The concentration versus time curve could be fit very well to $\sqrt{t}$ behavior. TEM image analysis allowed the measurement of mean flake thickness, $\langle\tau\rangle$, as well as mean flakes length and width, $\langle L\rangle$ and $\langle w\rangle$ as a function of time. This showed that the dispersions consisted of few layer graphene at all times with $\langle\tau\rangle$ equivalent to three layers for all times. However, as sonication time increased, the flake width and length decreased as $t^{-1/2}$ as observed previously for nanotubes.[136] This behavior can be used to explain the scaling of concentration with $\sqrt{t}$. We propose that the maximum concentration is that where the average solvent volume per flake is just the sphere defined by the flake length. Such behavior is observed in dispersions of SWNTs in NMP[59] and is related to the concept of pervaded volume in polymer physics.[48] In this scenario, the concentration is given by:

$$C_G \approx \frac{\rho_G \langle L\rangle\langle w\rangle\langle\tau\rangle}{4\pi\langle L/2\rangle^3/3} \approx \frac{6\rho_G}{\pi}\frac{\langle w\rangle\langle\tau\rangle}{\langle L\rangle^2} \propto \sqrt{t} \qquad (16)$$

where ρ_G is the graphitic density (2 200 kg m^{-3}). As shown by the dashed line in Figure 12, this expression allows near perfect reproduction of the graphitic concentration at all times without the need for any adjustable parameters.

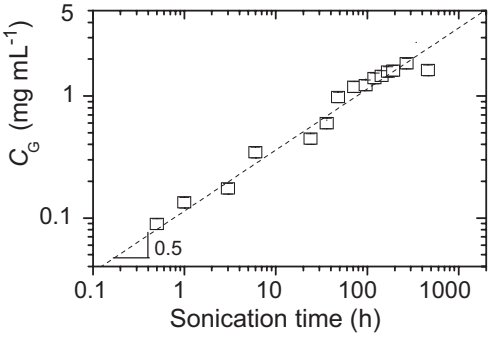

Figure 12. Concentration of graphene after centrifugation as a function of sonication time. The line illustrates $\sqrt{t}$ behavior.

This work is important because it shows that not only can graphite be exfoliated to give graphene in common solvents, but such dispersions can be produced at extremely high concentrations. This brings graphene dispersions to the point where they are useful for many applications.

8.2. Surfactants

However, many applications are ruled out by the need to use high boiling point, relatively toxic solvents such as NMP. A much better solution would be to exfoliate graphene in a low boiling point, benign solvent such as water. However, water does not fulfill the surface energy criteria (close to 40 mJ m^{-2}) required of a graphene solvent. However, by analogy to the approaches described above to disperse nanotubes, one could imagine using surfactants or DNA to disperse and exfoliate graphene.

We have attempted both of these methods. We found that genomic DNA (salmon sperm) does not successfully disperse graphene. This is perhaps unsurprising as the DNA interaction with a planar surface would be considerably different to that with a nanotube. However, we achieved more success with surfactants.

We sonicated graphite powder in aqueous solutions of sodium dodecylbenzene sulphonate (SDBS).[137] After mild centrifugation, we obtained a gray dispersion with graphene concentration approaching 0.1 mg mL^{-1}. TEM analysis showed the presence of large quantities of few layer graphene. These flakes ranged in size from 100 nm to 3 μm. While typical flakes consisted of 3–5 layers, a small number of monolayers were observed. The monolayers were of high quality with HRTEM clearing showing the hexagonal graphitic lattice. Both Fourier transform infrared and X-ray photoelectron spectroscopy showed virtually no evidence of oxides, while Raman spectroscopy showed a small defect content, consistent with flake edges. These dispersed flakes are relatively stable against aggregation and sedimentation although larger flakes tend to fall out over days. That the flakes are dispersed in an aqueous environment greatly facilitates processing. For example, individual flakes can be deposited on substrates by spraying. In addition, films can be formed on cellulose membranes by vacuum filtration.[138] These films have interesting optical and electrical

properties. They display transparencies of up to 90% and DC conductivity of up to 1.5×10^4 S m^{-1}.

9. Conclusions

Since 2006 we have carried out research in most areas of nanotube dispersion and stabilization: dispersion in solvents, with the aid of surfactants or biomolecules and by functionalization. In all cases we have attempted to quantitatively measure the dispersion quality and have reported it using a small number of well defined metrics. By comparing the metrics for the varying dispersant types, we conclude that functionalization gives the highest populations of individual nanotubes. In addition, in each case we have explored the mechanisms of dispersion. In some cases this has allowed us to make predictions which have lead to improved dispersion.

We found that for all systems studied, the dispersion quality increases as the concentration decreases. This allows the optimization of dispersion quality by measured dilution. The advantage of this is that loss of nanotubes is minimized, especially in systems such as CHP where very few aggregates are formed. However the disadvantage of this technique is that the dispersion quality never matches that achieved by ultracentrifugation.

In studying the mechanisms of dispersion we have made a number of interesting observations. For nanotubes dispersed in solvents, the solvent quality is determined by well-defined solubility parameters. Both traditional Hildebrand and Hansen solubility parameters, based on cohesive energies, and newer solubility parameters based on surface energies work very well. In fact it was the prediction that successful solvents had surface tension close to 70 mJ m^{-2} that lead to the discovery of a number of new solvents, including CHP. Similarly, for functionalized nanotubes we find that good solvents are those with Hildebrand solubility parameters which match the solubility parameters of the functional group. In addition, for surfactant dispersions, we have demonstrated the link between dispersion quality and zeta potential. This has allowed us to describe the ideal surfactant for nanotubes as small molecules which pack tightly on the tube surface. Similarly we have shown that genomic, double-stranded DNA unzips in order to interact, strand by strand, wrapping tightly around the nanotube.

The importance of understanding dispersion mechanisms is nicely illustrated in the fact that discovery of the need for matching between solvent and nanotube surface energy has allowed the first large scale exfoliation of graphene. In addition, we have shown that our knowledge of surfactant exfoliation of nanotubes can be successfully transferred over to graphene.

We expect that the lessons learned over the last decade about the exfoliation of nanotubes will be applied to the dispersion of graphene by a number of groups. The goals here will be simple. The aggregation state of graphene will have to be improved, with the mean number of monolayers per flake approaching one. In addition, much larger flakes will have to be dispersed. Both of these conditions will have to be achieved at high concentration to be useful. This will be a challenge and both new dispersants and new processing methods will be required to achieve these goals. However, as mentioned, we are not starting from scratch. Building on our understanding of nanotube exfoliation, I believe progress will be extremely rapid.

The study of dispersion and exfoliation of nanostructures is not just an academic area of physical chemistry, although it is rich in both the physics and chemistry of the liquid phase. It is important as an enabling technology for a whole array of research. The first studies of optical properties of nanotubes could not have been performed without the ability to exfoliate nanotubes in the liquid phase. Neither would the first demonstrations of ultra-strong composite fibers or transparent conducting films have been possible without the ability to produce high-quality dispersions. We feel that further development of nanotube dispersions, reaching higher levels of exfoliation at high concentrations, may very well facilitate new discoveries. Indeed, the demonstration of liquid phase exfoliation of graphene may be the key to the practical realization of graphene's wonderful properties. It looks like dispersion studies could be central to many areas of nanoscience for years to come.

Acknowledgements

I would like to acknowledgment SFI funding under the PI award scheme, contract number 07/IN.1/I1772. In addition, I must thank all those within my group who contributed to this work. It is impossible to mention you all but special thanks must go to Dr Shane Bergin and Dr Valeria Nicolosi.

Received: September 1, 2009
Published online: November 11, 2009

[1] R. H. Baughman, A. A. Zakhidov, W. A. de Heer, *Science* **2002**, *297*, 787.
[2] A. K. Geim, *Science* **2009**, *324*, 1530.
[3] A. K. Geim, K. S. Novoselov, *Nat. Mater.* **2007**, *6*, 183.
[4] M. Yu, O. Lourie, M. J. Dyer, T. F. Kelly, R. S. Ruoff, *Science* **2000**, *287*, 637.
[5] J. N. Coleman, U. Khan, Y. K. Gun'ko, *Adv. Mater.* **2006**, *18*, 689.
[6] B. Q. Wei, R. Vajtai, P. M. Ajayan, *Appl. Phys. Lett.* **2001**, *79*, 1172.
[7] P. Kim, L. Shi, A. Majumdar, P. L. McEuen, *Phys. Rev. Lett.* **2001**, 8721.
[8] J. W. Che, T. Cagin, W. A. Goddard, *Nanotechnology* **2000**, *11*, 65.
[9] M. A. Osman, D. Srivastava, *Nanotechnology* **2001**, *12*, 21.
[10] S. Berber, Y. Kwon, D. Tománek, *Phys. Rev. Lett.* **2000**, *84*, 4613.
[11] B. M. Kim, A. M. S. Fuhrer, *J. Phys.: Condens. Matter* **2004**, *16*, R553.
[12] A. Bachtold, P. Hadley, T. Nakanishi, C. Dekker, *Science* **2001**, *294*, 1317.
[13] A. Javey, J. Guo, Q. Wang, M. Lundstrom, H. J. Dai, *Nature* **2003**, *424*, 654.
[14] A. Kis, D. Mihailovic, M. Remskar, A. Mrzel, A. Jesih, I. Piwonski, A. J. Kulik, W. Benoit, L. Forro, *Adv. Mater.* **2003**, *15*, 733.
[15] J. P. Salvetat, G. A. D. Briggs, J. M. Bonard, R. R. Bacsa, A. J. Kulik, T. Stockli, N. A. Burnham, L. Forro, *Phys. Rev. Lett.* **1999**, *82*, 944.
[16] K. D. Ausman, R. Piner, O. Lourie, R. S. Ruoff, M. Korobov, *J. Phys. Chem. B* **2000**, *104*, 8911.
[17] J. L. Bahr, E. T. Mickelson, M. J. Bronikowski, R. E. Smalley, J. M. Tour, *Chem. Commun.* **2001**, 193.
[18] S. D. Bergin, V. Nicolosi, P. V. Streich, S. Giordani, Z. Sun, A. H. Windle, P. Ryan, N. Peter, P. Niraj, Z.-T. T. Wang, L. Carpenter, W. J. Blau, J. J. Boland, J. P. Hamilton, J. N. Coleman, *Adv. Mater.* **2008**, *20*, 1876.
[19] S. D. Bergin, Z. Y. Sun, D. Rickard, P. V. Streich, J. P. Hamilton, J. N. Coleman, *ACS Nano* **2009**, *3*, 2340.
[20] S. Detriche, G. Zorzini, J. F. Colomer, A. Fonseca, J. B. Nagy, *J. Nanosci. Nanotechnol.* **2007**, *8*, 6082.
[21] C. A. Furtado, U. J. Kim, H. R. Gutierrez, L. Pan, E. C. Dickey, P. C. Eklund, *J. Am. Chem. Soc.* **2004**, *126*, 6095.
[22] B. J. Landi, H. J. Ruf, J. J. Worman, R. P. Raffaelle, *J. Phys. Chem. B* **2004**, *108*, 17089.
[23] Y. Maeda, S. Kimura, Y. Hirashima, M. Kanda, Y. F. Lian, T. Wakahara, T. Akasaka, T. Hasegawa, H. Tokumoto, T. Shimizu, H. Kataura,

Y. Miyauchi, S. Maruyama, K. Kobayashi, S. Nagase, *J. Phys. Chem. B* **2004**, *108*, 18395.
[24] Q. Xiao, P. H. Wang, Z. C. Si, *Prog. Chem.* **2007**, *19*, 101.
[25] V. A. Davis, L. M. Ericson, A. N. G. Parra-Vasquez, H. Fan, Y. H. Wang, V. Prieto, J. A. Longoria, S. Ramesh, R. K. Saini, C. Kittrell, W. E. Billups, W. W. Adams, R. H. Hauge, R. E. Smalley, M. Pasquali, *Macromolecules* **2004**, *37*, 154.
[26] S. Ramesh, L. M. Ericson, V. A. Davis, R. K. Saini, C. Kittrell, M. Pasquali, W. E. Billups, W. W. Adams, R. H. Hauge, R. E. Smalley, *J. Phys. Chem. B* **2004**, *108*, 8794.
[27] M. Cadek, J. N. Coleman, K. P. Ryan, V. Nicolosi, G. Bister, A. Fonseca, J. B. Nagy, K. Szostak, F. Beguin, W. J. Blau, *Nano Lett.* **2004**, *4*, 353.
[28] A. B. Dalton, C. Stephan, J. N. Coleman, B. McCarthy, P. M. Ajayan, S. Lefrant, P. Bernier, W. J. Blau, H. J. Byrne, *J. Phys. Chem. B* **2000**, *104*, 10012.
[29] B. McCarthy, J. N. Coleman, S. A. Curran, A. B. Dalton, A. P. Davey, Z. Konya, A. Fonseca, J. B. Nagy, W. J. Blau, *J. Mater. Sci. Lett.* **2000**, *19*, 2239.
[30] R. Murphy, J. N. Coleman, M. Cadek, B. McCarthy, M. Bent, A. Drury, R. C. Barklie, W. J. Blau, *J. Phys. Chem. B* **2002**, *106*, 3087.
[31] L. Vaisman, H. D. Wagner, G. Marom, *Adv. Colloid Interface Sci.* **2006**, *128*, 37.
[32] H. Wang, W. Zhou, D. L. Ho, K. I. Winey, J. E. Fischer, C. J. Glinka, E. K. Hobbie, *Nano Lett.* **2004**, *4*, 1789.
[33] G. S. Duesberg, M. Burghard, J. Muster, G. Philipp, S. Roth, *Chem. Commun.* **1998**, 435.
[34] M. J. O'Connell, S. M. Bachilo, C. B. Huffman, V. C. Moore, M. S. Strano, E. H. Haroz, K. L. Rialon, P. J. Boul, W. H. Noon, C. Kittrell, J. P. Ma, R. H. Hauge, R. B. Weisman, R. E. Smalley, *Science* **2002**, *297*, 593.
[35] B. Zhao, H. Hu, A. P. Yu, D. Perea, R. C. Haddon, *J. Am. Chem. Soc.* **2005**, *127*, 8197.
[36] R. Blake, Y. K. Gun'ko, J. Coleman, M. Cadek, A. Fonseca, J. B. Nagy, W. J. Blau, *J. Am. Chem. Soc.* **2004**, *126*, 10226.
[37] V. Zorbas, A. Ortiz-Acevedo, A. B. Dalton, M. M. Yoshida, G. R. Dieckmann, R. K. Draper, R. H. Baughman, M. Jose-Yacaman, I. H. Musselman, *J. Am. Chem. Soc.* **2004**, *126*, 7222.
[38] M. S. Arnold, A. A. Green, J. F. Hulvat, S. I. Stupp, M. C. Hersam, *Nat. Nanotechnol.* **2006**, *1*, 60.
[39] M. S. Arnold, S. I. Stupp, M. C. Hersam, *Nano Lett.* **2005**, *5*, 713.
[40] X. M. Tu, S. Manohar, A. Jagota, M. Zheng, *Nature* **2009**, *460*, 250.
[41] Y. Hernandez, V. Nicolosi, M. Lotya, F. M. Blighe, Z. Y. Sun, S. De, I. T. McGovern, B. Holland, M. Byrne, Y. K. Gun'ko, J. J. Boland, P. Niraj, G. Duesberg, S. Krishnamurthy, R. Goodhue, J. Hutchison, V. Scardaci, A. C. Ferrari, J. N. Coleman, *Nat. Nanotechnol.* **2008**, *3*, 563.
[42] M. Lotya, Y. Hernandez, P. J. King, R. J. Smith, V. Nicolosi, L. S. Karlsson, F. M. Blighe, S. De, Z. M. Wang, I. T. McGovern, G. S. Duesberg, J. N. Coleman, *J. Am. Chem. Soc.* **2009**, *131*, 3611.
[43] P. Blake, P. D. Brimicombe, R. R. Nair, T. J. Booth, D. Jiang, F. Schedin, L. A. Ponomarenko, S. V. Morozov, Hn. F. Gleeson, E. W. Hill, A. K. Geim, K. S. Novoselov, *Nano Lett.* **2008**, *8*, 1704.
[44] A. B. Bourlinos, V. Georgakilas, R. Zboril, T. A. Steriotis, A. K. Stubos, *Small* **2009**, *5*, 1841.
[45] J. Israelachvili, *Intermolecular and Surface Forces*, Academic Press, London **1991**.
[46] C. M. Hansen, *Hansen Solubility Parameters - A User's Handbook*, CRC Press, Boca Raton, FL **2007**.
[47] J. H. Hildebrand, J. M. Prausnitz, R. L. Scott, *Regular and Related Solutions*, Van Nostrand Reinhold Company, New York **1970**.
[48] M. Rubinstein, R. H. Colby, *Polymer Physics*, Oxford University Press, Oxford **2003**.
[49] A. D. McLachlan, *Discuss. Faraday Soc.* **1965**, 239.
[50] R. J. Hunter, *Introduction to Modern Colloid Science*, Oxford Science Publications, Oxford **1994**.
[51] D. Chapot, L. Bocquet, E. Trizac, *J. Colloid Interface Sci.* **2005**, *285*, 609.
[52] Z. Sun, V. Nicolosi, D. Rickard, S. D. Bergin, D. Aherne, J. N. Coleman, *J. Phys. Chem. C* **2008**, *112*, 10692.
[53] R. Krupke, F. Hennrich, O. Hampe, M. M. Kappes, *J. Phys. Chem. B* **2003**, *107*, 5667.
[54] J. Liu, M. J. Casavant, M. Cox, D. A. Walters, P. Boul, W. Lu, A. J. Rimberg, K. A. Smith, D. T. Colbert, R. E. Smalley, *Chem. Phys. Lett.* **1999**, *303*, 125.
[55] P. Umek, D. Vrbanic, M. Remskar, T. Mertelj, P. Venturini, S. Pejovnik, D. Mihailovic, *Carbon* **2002**, *40*, 2581.
[56] H. T. Ham, Y. S. Choi, I. J. Chung, *J. Colloid Interface Sci.* **2005**, *286*, 216.
[57] M. S. Strano, V. C. Moore, M. K. Miller, M. J. Allen, E. H. Haroz, C. Kittrell, R. H. Hauge, R. E. Smalley, *J. Nanosci. Nanotechnol.* **2003**, *3*, 81.
[58] S. D. Bergin, V. Nicolosi, S. Giordani, A. de Gromard, L. Carpenter, W. J. Blau, J. N. Coleman, *Nanotechnology* **2007**, *18*, 455705.
[59] S. Giordani, S. D. Bergin, V. Nicolosi, S. Lebedkin, M. M. Kappes, W. J. Blau, J. N. Coleman, *J. Phys. Chem. B* **2006**, *110*, 15708.
[60] S. J. Zhang, I. A. Kinloch, A. H. Windle, *Nano Lett.* **2006**, *6*, 568.
[61] P. J. Flory, *Principles of Polymer Chemistry*, Cornell University Press, Ithica, NY **1953**.
[62] P. J. Flory, *Proc. R. Soc. of London, Ser. A* **1956**, *234*, 60.
[63] S. D. Bergin, Z. Sun, P. V. Streich, J. Hamilton, J. N. Coleman, *J. Phys. Chem. C*, in press.
[64] Z. Y. Sun, I. O'Connor, S. D. Bergin, J. N. Coleman, *J. Phys. Chem. C* **2009**, *113*, 1260.
[65] J. A. Fagan, J. R. Simpson, B. J. Landi, L. J. Richter, I. Mandelbaum, V. Bajpai, D. L. Ho, R. Raffaelle, A. R. H. Walker, B. J. Bauer, E. K. Hobbie, *Phys. Rev. Lett.* **2007**, *98*, 4.
[66] A. Beerbower, *J. Colloid Interface Sci.* **1971**, *35*, 126.
[67] D. M. Koenhen, C. A. Smolders, *J. Appl. Polym. Sci.* **1975**, *19*, 1163.
[68] M. Grujicic, G. Cao, W. N. Roy, *J. Mater. Sci.* **2004**, *39*, 2315.
[69] H. Cathcart, J. N. Coleman, *Chem. Phys. Lett.* **2009**, *474*, 122.
[70] H. Cathcart, S. Quinn, V. Nicolosi, J. M. Kelly, W. J. Blau, J. N. Coleman, *J. Phys. Chem. C* **2007**, *111*, 66.
[71] J. Crochet, M. Clemens, T. Hertel, *J. Am. Chem. Soc.* **2007**, *129*, 8058.
[72] V. Nicolosi, D. N. McCarthy, D. Vengust, D. Mihailovic, W. J. Blau, J. N. Coleman, *Eur. Phys. J.: Appl. Phys.* **2007**, *37*, 149.
[73] V. Nicolosi, D. Vengust, D. Mihailovic, W. J. Blau, J. N. Coleman, *Chem. Phys. Lett.* **2006**, *425*, 89.
[74] T. Hasan, V. Scardaci, P. H. Tan, A. G. Rozhin, W. I. Milne, A. C. Ferrari, *J. Phys. Chem. C* **2007**, *111*, 12594.
[75] S. Bandow, A. M. Rao, K. A. Williams, A. Thess, R. E. Smalley, P. C. Eklund, *J. Phys. Chem. B* **1997**, *101*, 8839.
[76] J. M. Bonard, T. Stora, J. P. Salvetat, F. Maier, T. Stockli, C. Duschl, L. Forro, W. A. deHeer, A. Chatelain, *Adv. Mater.* **1997**, *9*, 827.
[77] G. S. Duesberg, J. Muster, V. Krstic, M. Burghard, S. Roth, *Appl. Phys. A: Mater. Sci. Process.* **1998**, *67*, 117.
[78] J. Liu, A. G. Rinzler, H. J. Dai, J. H. Hafner, R. K. Bradley, P. J. Boul, A. Lu, T. Iverson, K. Shelimov, C. B. Huffman, F. Rodriguez-Macias, Y. S. Shon, T. R. Lee, D. T. Colbert, R. E. Smalley, *Science* **1998**, *280*, 1253.
[79] B. Vigolo, A. Penicaud, C. Coulon, C. Sauder, R. Pailler, C. Journet, P. Bernier, P. Poulin, *Science* **2000**, *290*, 1331.
[80] C. Y. Hu, Y. J. Xu, S. W. Duo, R. F. Zhang, M. S. Li, *J. Chin. Chem. Soc.* **2009**, *56*, 234.
[81] V. C. Moore, M. S. Strano, E. H. Haroz, R. H. Hauge, R. E. Smalley, J. Schmidt, Y. Talmon, *Nano Lett.* **2003**, *3*, 1379.
[82] M. F. Islam, E. Rojas, D. M. Bergey, A. T. Johnson, A. G. Yodh, *Nano Lett.* **2003**, *3*, 269.
[83] S. M. Bachilo, M. S. Strano, C. Kittrell, R. H. Hauge, R. E. Smalley, R. B. Weisman, *Science* **2002**, *298*, 2361.
[84] D. A. Tsyboulski, S. M. Bachilo, R. B. Weisman, *Nano Lett.* **2005**, *5*, 975.
[85] E. M. Doherty, S. De, P. E. Lyons, A. Shmeliov, P. N. Nirmalraj, V. Scardaci, J. Joimel, W. J. Blau, J. J. Boland, J. N. Coleman, *Carbon* **2009**, *47*, 2466.
[86] L. Hu, D. S. Hecht, G. Gruner, *Nano Lett.* **2004**, *4*, 2513.
[87] H. Z. Geng, D. S. Lee, K. K. Kim, G. H. Han, H. K. Park, Y. H. Lee, *Chem. Phys. Lett.* **2008**, *455*, 275.

[88] S. D. Bergin, V. Nicolosi, H. Cathcart, M. Lotya, D. Rickard, Z. Y. Sun, W. J. Blau, J. N. Coleman, *J. Phys. Chem. C* **2008**, *112*, 972.
[89] T. J. McDonald, C. Engtrakul, M. Jones, G. Rumbles, M. J. Heben, *J. Phys. Chem. B* **2006**, *110*, 25339.
[90] D. Rickard, S. Giordam, W. Blau, J. N. Coleman, *J. Lumin.* **2008**, *128*, 31.
[91] B. White, S. Banerjee, S. O'Brien, N. J. Turro, I. P. Herman, *J. Phys. Chem. C* **2007**, *111*, 13684.
[92] M. S. Arnold, J. Suntivich, S. I. Stupp, M. C. Hersam, *ACS Nano* **2008**, *2*, 2291.
[93] M. J. O'Connell, P. Boul, L. M. Ericson, C. Huffman, Y. H. Wang, E. Haroz, C. Kuper, J. Tour, K. D. Ausman, R. E. Smalley, *Chem. Phys. Lett.* **2001**, *342*, 265.
[94] H. Cathcart, S. Quinn, V. Nicolosi, J. M. Kelly, W. J. Blau, J. N. Coleman, *J. Phys. Chem. C* **2007**, *111*, 66.
[95] B. Gigliotti, B. Sakizzie, D. S. Bethune, R. M. Shelby, J. N. Cha, *Nano Lett.* **2006**, *6*, 159.
[96] N. Nakashima, S. Okuzono, H. Murakami, T. Nakai, K. Yoshikawa, *Chem. Lett.* **2003**, *32*, 456.
[97] M. Zheng, A. Jagota, E. D. Semke, B. A. Diner, R. S. McLean, S. R. Lustig, R. E. Richardson, N. G. Tassi, *Nat. Mater.* **2003**, *2*, 338.
[98] M. Zheng, A. Jagota, M. S. Strano, A. P. Santos, P. Barone, S. G. Chou, B. A. Diner, M. S. Dresselhaus, R. S. McLean, G. B. Onoa, G. G. Samsonidze, E. D. Semke, M. Usrey, D. J. Walls, *Science* **2003**, *302*, 1545.
[99] R. J. Chen, Y. Zhang, *J. Phys. Chem. B* **2006**, *110*, 54.
[100] D. A. Heller, S. Baik, T. E. Eurell, M. S. Strano, *Adv. Mater.* **2005**, *17*, 2793.
[101] M. S. Arnold, S. I. Stupp, M. C. Hersam, *Nano Lett.* **2005**, *5*, 713.
[102] J. N. Barisci, M. Tahhan, G. G. Wallace, S. Badaire, T. Vaugien, M. Maugey, P. Poulin, *Adv. Funct. Mater.* **2004**, *14*, 133.
[103] K. Keren, R. S. Berman, E. Buchstab, U. Sivan, E. Braun, *Science* **2003**, *302*, 1380.
[104] E. K. Hobbie, B. J. Bauer, J. Stephens, M. L. Becker, P. McGuiggan, S. D. Hudson, H. Wang, *Langmuir* **2005**, *21*, 10284.
[105] C. Staii, A. T. Johnson, M. Chen, A. Gelperin, *Nano Lett.* **2005**, *5*, 1774.
[106] D. A. Heller, E. S. Jeng, Y. Tsun-Kwan, B. M. Martinez, A. E. Moll, J. B. Gastala, M. S. Strano, *Science* **2006**, *311*, 508.
[107] C. Hu, Y. Zhang, G. Bao, Y. Zhang, M. Liu, Z. L. Wang, *J. . Phys. Chem. B* **2005**, *109*, 20072.
[108] V. A. Karachevtsev, A. Y. Glamazda, V. S. Leontiev, O. S. Lytvyn, U. Dettlaff-Weglikowska, *Chem. Phys. Lett.* **2007**, *435*, 104.
[109] K. S. Rao, S. Daniel, T. P. Rao, S. U. Rani, G. R. K. Naidu, L. Hea-Yeon, T. Kawai, *Sens. Actuators, B* **2007**, *122*, 672.
[110] H. Cathcart, V. Nicolosi, J. M. Hughes, W. J. Blau, J. M. Kelly, S. J. Quinn, J. N. Coleman, *J. Am. Chem. Soc.* **2008**, *130*, 12734.
[111] V. Nicolosi, H. Cathcart, A. R. Dalton, D. Aherne, G. R. Dieckmann, J. N. Coleman, *Biomacromolecules* **2008**, *9*, 598.
[112] R. R. Johnson, A. T. C. Johnson, M. L. Klein, *Nano Lett.* **2008**, *8*, 69.
[113] G. Dukovic, B. E. White, Z. Zhou, F. Wang, S. Jockusch, M. L. Steigerwald, T. F. Heinz, R. A. Friesner, N. J. Turro, L. E. Brus, *J. Am. Chem. Soc.* **2004**, *126*, 15269.
[114] M. S. Strano, C. B. Huffman, V. C. Moore, M. J. O'Connell, E. H. Haroz, J. Hubbard, M. Miller, K. Rialon, C. Kittrell, S. Ramesh, R. H. Hauge, R. E. Smalley, *J. Phys. Chem. B* **2003**, *107*, 6979.
[115] S. Banerjee, T. Hemraj-Benny, S. S. Wong, *Adv. Mater.* **2005**, *17*, 17.
[116] S. Niyogi, M. A. Hamon, H. Hu, B. Zhao, P. Bhowmik, R. Sen, M. E. Itkis, R. C. Haddon, *Acc. Chem. Res.* **2002**, *35*, 1105.
[117] R. A. L. Jones, *Soft Condensed Matter*, Oxford University Press, Oxford **2002**.
[118] A. Penicaud, P. Poulin, A. Derre, E. Anglaret, P. Petit, *J. Am. Chem. Soc.* **2005**, *127*, 8.
[119] J. Amiran, V. Nicolosi, S. D. Bergin, U. Khan, P. E. Lyons, J. N. Coleman, *J. Phys. Chem. C* **2008**, *112*, 3519.
[120] C. Lee, X. D. Wei, J. W. Kysar, J. Hone, *Science* **2008**, *321*, 385.
[121] K. S. Novoselov, A. K. Geim, S. V. Morozov, D. Jiang, Y. Zhang, S. V. Dubonos, I. V. Grigorieva, A. A. Firsov, *Science* **2004**, *306*, 666.
[122] A. A. Balandin, S. Ghosh, W. Z. Bao, I. Calizo, D. Teweldebrhan, F. Miao, C. N. Lau, *Nano Lett.* **2008**, *8*, 902.
[123] K. S. Novoselov, D. Jiang, F. Schedin, T. J. Booth, V. V. Khotkevich, S. V. Morozov, A. K. Geim, *Proc. Natl. Acad. Sci. U. S. A.* **2005**, *102*, 10451.
[124] R. Ruoff, *Nat. Nanotechnol.* **2008**, *3*, 10.
[125] S. Stankovich, D. A. Dikin, G. H. B. Dommett, K. M. Kohlhaas, E. J. Zimney, E. A. Stach, R. D. Piner, S. T. Nguyen, R. S. Ruoff, *Nature* **2006**, *442*, 282.
[126] S. Stankovich, R. D. Piner, X. Q. Chen, N. Q. Wu, S. T. Nguyen, R. S. Ruoff, *J. Mater. Chem.* **2006**, *16*, 155.
[127] D. Li, M. B. Muller, S. Gilje, R. B. Kaner, G. G. Wallace, *Nat. Nanotechnol.* **2008**, *3*, 101.
[128] S. Stankovich, D. A. Dikin, R. D. Piner, K. A. Kohlhaas, A. Kleinhammes, Y. Jia, Y. Wu, S. T. Nguyen, R. S. Ruoff, *Carbon* **2007**, *45*, 1558.
[129] G. Eda, G. Fanchini, M. Chhowalla, *Nat. Nanotechnol.* **2008**, *3*, 270.
[130] C. Gomez-Navarro, R. T. Weitz, A. M. Bittner, M. Scolari, A. Mews, M. Burghard, K. Kern, *Nano Lett.* **2007**, *7*, 3499.
[131] H. Kang, A. Kulkarni, S. Stankovich, R. S. Ruoff, S. Baik, *Carbon* **2009**, *47*, 1520.
[132] K. N. Kudin, B. Ozbas, H. C. Schniepp, R. K. Prud'homme, I. A. Aksay, R. Car, *Nano Lett.* **2008**, *8*, 36.
[133] D. Yang, A. Velamakanni, G. Bozoklu, S. Park, M. Stoller, R. D. Piner, S. Stankovich, I. Jung, D. A. Field, C. A. Ventrice, R. S. Ruoff, *Carbon* **2009**, *47*, 145.
[134] S. Horiuchi, T. Gotou, M. Fuijwara, R. Sotoaka, M. Hirata, K. Kimoto, T. Asaka, T. Yokosawa, Y. Matsui, K. Watanabe, M. Sekita, *Japan. J. Appl. Phys, Part 2*, **2003**, *42*, L1073.
[135] U. Khan, A. O'Neill, M. Lotya, S. De, J. N. Coleman, unpublished.
[136] F. Hennrich, R. Krupke, K. Arnold, J. A. Rojas Stutz, S. Lebedkin, T. Koch, T. Schimmel, M. M. Kappes, *J. Phys. Chem. B* **2007**, *111*, 1932.
[137] M. Lotya, Y. Hernandez, P. J. King, R. J. Smith, V. Nicolosi, L. S. Karlsson, F. M. Blighe, S. De, Z. Wang, I. T. McGovern, G. S. Duesberg, J. N. Coleman, *J. Am. Chem. Soc.* **2009**, *131*, 3611.
[138] S. De, P. J. King, M. Lotya, A. O'Neill, E. M. Doherty, Y. Hernandez, G. S. Duesberg, J. N. Coleman, *Small*, in press.